Enhancing the Urban Resilience to Flood Risk Through a Decision Support Tool for the LID-BMPs Optimal Design

Francesco Pugliese[1] 🔘 · **Carlo Gerundo[2]** · **Francesco De Paola[1]** · **Gerardo Caroppi[3]** · **Maurizio Giugni[1]**

Abstract

Urban areas are becoming increasingly susceptible to flooding because of high urbanization levels and changes in the precipitation patterns caused by climate change. The effective management of urban water drainage systems is particularly relevant to control and regulate the runoff impacts. Nevertheless, the mitigation of climate change effects and the adaptation to its impacts call for the implementation of new sustainable strategies and solutions. In this context, a key role can be played by Low Impact Development (LID) technologies of Best Management Practices (BMPs). Such innovative design approaches can lead to more sustainable and effective strategies for urban runoff control. In this paper, a methodology to increase the urban resilience to flooding risk through LID-BMPs is proposed and discussed. A tool for the optimal selection and design of different LID-BMPs is presented. The tool couples GIS processing with hydraulic simulations, constituting a Decision Support System (DSS) based on the meta-heuristic optimization algorithm Harmony Search (HS). The methodology was tested on the case study site of Soccavo, a suburban area in the Municipality of Naples (Italy). Several LID measures, including bio-retention systems, porous pavements, green roofs, were considered. Then, the effectiveness of combining LIDs with grey solutions to carry out hybrid solutions was also assessed. Results showed the capability of the proposed approach in detecting technically and economically viable solutions.

1 Introduction

Climate change is emerging as one of the distinguishing features of the early 21st Century (Carter et al. 2015). It is producing, along with the uncontrolled and unregulated soil exploitation, increasingly frequent and intense natural phenomena such as droughts, heat waves and flooding (Rosenzweig et al. 2015). In the last two decades, European Union

✉ Francesco Pugliese
    francesco.pugliese2@unina.it

Extended author information available on the last page of the article

(EU) has become a leader in international climate change politics (Schreurs and Tiberghien 2007; Wurzel and Connelly 2010), paying increasing attention to the crucial role that cities could play in addressing the climatic, environmental and socio-economic hurdles that European territories are constantly forced to experience. To deal with climate change effects, the employment of low-impact approaches is sparking interest in both urban (De Paola et al. 2018) and mountainous or rural areas (Pugliese et al. 2022; Pignalosa et al. 2022).

With specific reference to urban flood phenomena, also known as flash floods (Špitalar et al. 2014), the implementation of proper forecasting and prevention models (such as Early Warning and Early Safety Systems) is based on the application of predictive simulation models to enhance the tutelage from vulnerability and the risk exposure. In this context, the development of mitigation models and adaptive approaches, aimed at addressing the effects of flooding events at the urban scale, is pivotal for the management of urban rainwater infrastructures.

Many studies highlighted how the change in land use and the increase in impervious surfaces (deriving from the construction of buildings, parking areas and roads) are causing extreme floods in urban areas, with negative outcomes also on the resulting runoff water quality (Khan et al. 2006; Dietz 2007). The increasing urbanization negatively affects the surface runoff coefficients and induces changes in the urban hydrological cycle (Booth 1991), with implications on human safety and water resources.

To date, a large body of studies has investigated the influence of climate change on extreme rainfall events, specifically focusing on the implications for the design and management of water infrastructures (e.g. Nie et al. 2009; Forsee and Ahmad 2011; Fletcher et al. 2019). Nevertheless, still many constraints exist for the migration from the research outputs to the engineering practice. The technical effectiveness of the intervention, the related environmental, economic and social implications (Fletcher et al. 2015), along with the integration within the urban context, are thus an unresolved issue.

Among the design approaches aimed at increasing the performance of rainwater drainage systems and then, the urban resilience to flood risk, the technologies for the Low Impact Development of Best Management Practices (LID-BMPs) play a prevalent role. Such strategies seek to reduce and/or prevent adverse runoff impacts through sound site planning and both nonstructural and structural techniques that preserve or closely mimic the site's natural or pre-developed hydrologic response to precipitation (Blick et al. 2004).

LID-BMPs enhance the infiltration and evapotranspiration processes, by storing a rate of percolated inflow discharge to be then split into two rates: the former is conveyed to the sewer system (drain outflow) and the latter exfiltrates within the underlying soil layers (Fig. 1). Furthermore, these technologies can provide multiple benefits to the qualitive improvement of water, allowing for nutrient and pollutant removal.

Thus, LID-BMPs are potentially able to improve the flood control while inducing additional co-benefits in the urban environment (e.g. creating and enhancing green spaces). LID-BMPs provide new perspectives to the urban regeneration projects, although their design, and consequently their insertion in the urban tissue, need the development of multi-disciplinary approaches.

Structural LID practices include green roofs, draining trenches (infiltration trenches), porous pavements and vegetative swales. Each LID practice has different technical (polluting removal effectiveness, size, installation and maintenance costs, etc.) and non-technical (environmental impact, disposal capacity) features that make its selection and design a complex issue. Nevertheless, both these aspects are essential for the effective and sustainable management of rainwater in urban environments (You et al. 2019).
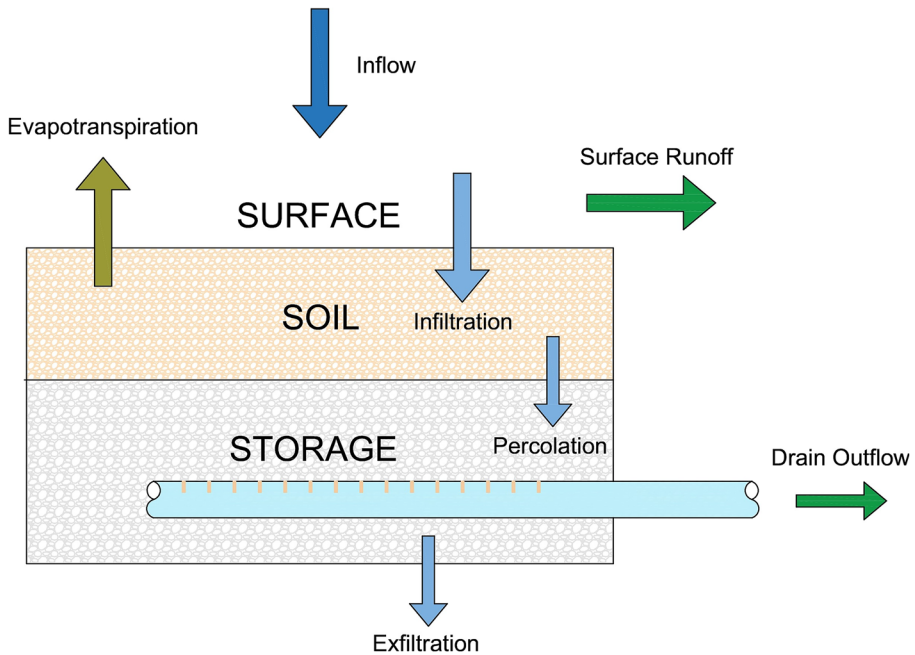
Fig. 1 Schematic representation of the hydrological processes of a LID

Several approaches have been proposed for the optimal LID-BMPs design and management in urban areas. Hou et al. (2020) implemented a multi-objective algorithm for the optimal spatial layout of LID-BMPs, to control the rainwater runoff, the peak discharge and the pollutants propagation in China. Jia et al. (2012) applied an optimization procedure, coupling the EPA SWMM 5.1 hydraulic solver (Rossman 2015) with the BMP Decision Support Tool (DSS), for the design of LID in the Olympic Village of Beijing (China), observing benefits in terms of reduction of both water volumes and peak flow of the sewer system. Liu et al. (2016) combined a hydrological model with an optimization algorithm for the selection and optimal location of LID in the urban catchment of Crooked Creek (USA), resulting in significant benefits in terms of effective outflows into the sewage system. Xu et al. (2017) combined the heuristic non-dominated sorting genetic algorithm (NSGA-II) with EPA SWMM 5.1 (Rossman 2015) hydraulic solver for the optimal selection among different LID scenarios in Tianjin (China), observing the reduction of both the peak flow and the pollutants load. Recanatesi et al. (2017) assessed the reduction of flood prone areas in a peri-urban watershed in Rome (Italy) deriving from the LID application. The complete removal of flooding risk was observed for the 90% of the area, whereas a significant reduction of exposed areas for the remaining 10%. Zanandrea and Silveira (2018) assessed the benefits from the implementation of LID practices in Brazil, with reference to four urbanization scenarios under different rainfall events. The peak flow reduction and delay resulted in a direct correlation with the forcing rainfall actions. Raei et al. (2019) proposed a multi-objective optimization framework, integrating a multi-layer perception neural network with a fuzzy technique and a decision-making model for supporting the acceptability and reliability of optimal LID management scenarios in Iran. De Paola et al. (2018) developed a DSS for the optimal design of LID in an urban environment. The effectiveness

of the tool was tested on two densely inhabited districts of Naples (Italy), showing specific flexibility in selecting the best technical solution, given the available economic budget. The model was based on the integration of the EPA SWMM 5.1 hydraulic solver with the Harmony Search (HS) meta-heuristic optimization algorithm (Geem et al. 2001), aimed at optimally designing LIDs in urban stormwater systems for controlling spilling and flooding events.

In the present work, on the basis of previous studies developed by the authors (De Paola et al. 2018), an optimal sizing methodology of LID-BMPs is discussed and tested on a real case, providing a novel tool to integrate the GIS spatial data processing with the Harmony Search meta-heuristic optimization model. The EPA SWMM 5.1 solver was applied for hydraulic simulations.

The methodology was tested on the case study of Soccavo, a densely inhabited district of the Municipality of Naples (Italy), presenting a high ratio of impervious to pervious areas, thus presenting a high vulnerability to flood risk provoked by extreme rainfall events.

Section 2 presents the methodological approach; Sect. 3 introduces the study area; in Sect. 4 the results are discussed, whereas in Sect. 5, the outcomes of the study are provided and the potential future developments of the research are discussed.

2 Methodological Approach

The methodological approach for the optimal design and location of LID-BMPs proposed in this study is aimed at enhancing urban resilience to extreme rainfall events. The proposed approach, schematically summarized in the flowchart of Fig. 2, was composed of six steps described in detail in the following sections.

2.1 Territorial Analysis

The first step of the methodology provided the detection of the data required for the LID-BMPs optimization in an urban catchment. The input data for the aforementioned simulations were: the catchment area A (m^2), its equivalent width W (m), estimated as the ratio between the catchment area and the maximum length of the drainage system trunks, the average slope s (%) assessed from a Digital Terrain Model (DTM) processing as the mean value of the catchment slope, and the rate of impervious surface $\%IMP$ (%), evaluated as the ratio between the impervious area and the total one.

The geographic database included vector data (land use, drainage network) and raster data (Digital terrain model, 3-band satellite imagery or orthophoto). The boundaries of the catchment and of its sub-catchments were delineated by processing a DTM with the *Hydrology toolbox* of the ArcGis 10.7 (ESRI 2010) environment. Then, the input data were processed using a novel in-house tool, according to the steps synthetically reported below.

2.1.1 Permeability Map Definition

A 3-band orthophoto was processed through a sequence of operations, performed with the software ArcGis Pro, briefly described in the following:

1. <u>Band extraction</u>, to split the impervious areas (buildings, roads, parking lots, other paved surfaces, etc.) from the pervious ones (vegetation, water bodies and bare soil), the
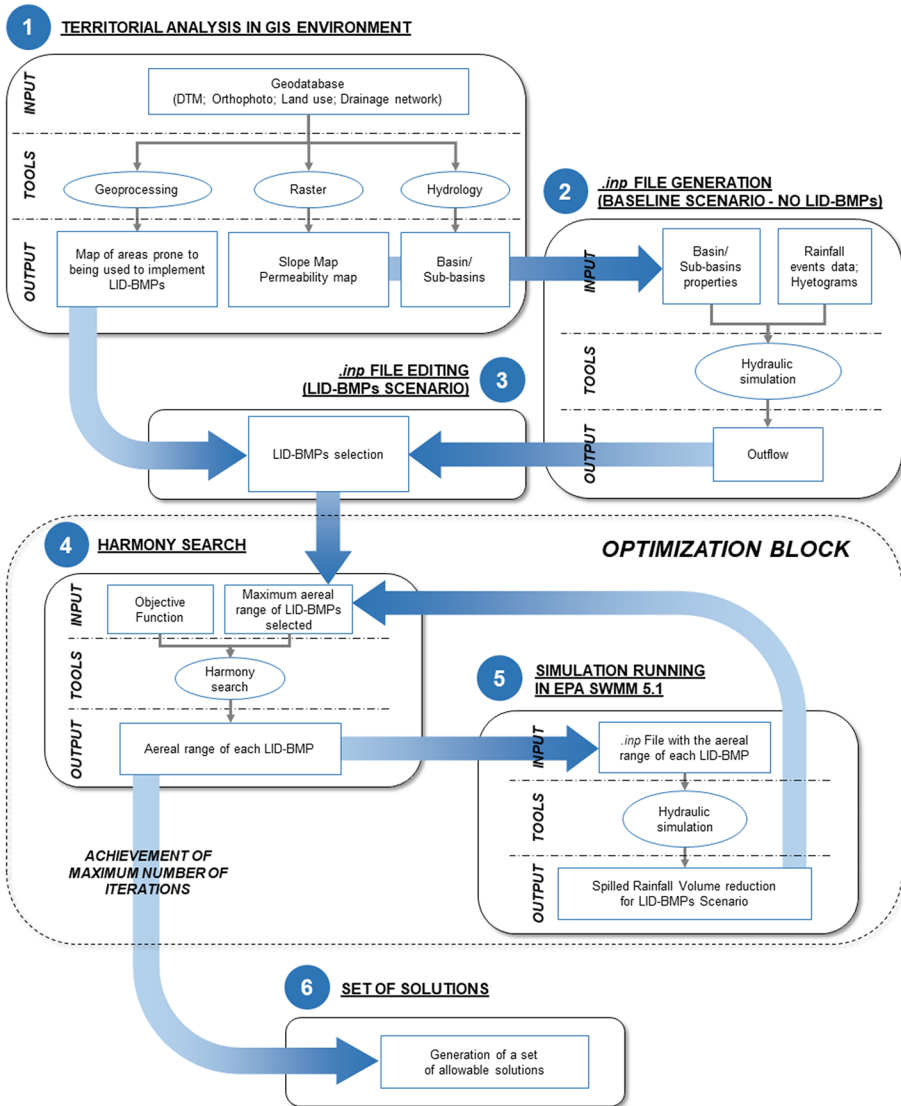
Fig. 2 Flowchart of the methodological approach for the optimal design and location of LID-BMPs

imageries were classified into different types of land use, by transforming the combination of bands to distinctly distinguish the spectral features. The spectral bands extracted included the Near Infrared (Band 4), emphasizing the vegetation; the Red (Band 1), highlighting the man-made objects and vegetation; and, finally, the Blue (Band 3), pointing the water bodies out.

2. Segmentation, to emphasize the differences between natural and anthropic areas in the imagery classification. It provided the pixel grouping into segments, aimed at limiting the number of spectral signatures to be classified. The optimal number of segments and

the range of adjacent pixels were grouped into a segment change, depending on both the image size and the desired detail of the classification.

3. <u>Classification</u>, to classify each segmented imagery of the Step 2) as pervious or impervious area.

4. <u>Reclassify errors</u>, to manually adjust the overlapping and inaccuracies of the automated classification of the segmented imagery, attributing to the misinterpreted segments the proper category (pervious/impervious).

5. <u>Validation</u>, to assess the classification accuracy through a statistical comparison between the classified imagery and the original one. A set of accuracy assessment *points* randomly scattered throughout the imagery was generated, in such a way as to be equally distributed between each class (pervious and impervious areas). The classified value of the image at each point location was compared with the current land-use type of the original image (ground truth).

6. <u>Confusion matrix computing</u>, to validate the accuracy assessment point and to generate the confusion matrix, comparing the classified attributes and defining the accuracy rate. The higher the number of correctly classified points, the greater the percentage in the confusion matrix, indicating a high accuracy of the classification.

The accuracy of classification was assessed through the *Kappa* index, calculated using the formula introduced by Bishop et al. (2007). The segmentation step was the most susceptible to generate the classification error, because if the fixed segmentation parameters detected the original image either as too heavy or too poor, several portions of the image were misclassified.

2.1.2 Automated Model for Urban Catchment Properties Calculation

The automated model for urban catchment or sub-catchment properties was composed of 3 sub-models:

1. *Slope computing*, returning the mean slope of the catchment/sub-catchment;
2. *Imperviousness rate computing*, processing the impervious map achieved by the orthophoto segmentation and classification, returning as output the impervious rate of the catchment/sub-catchment;
3. *Width computing*, processing the drainage network and providing the width of the catchment/sub-catchment.

2.1.3 Calculation of Maximum Areal Range of LID-BMPs

The size of each LID within the urban catchment was estimated by processing the land use map in a GIS environment.

Several factors affect the area convertible into a specific LID-BMP. Land use is certainly a pivotal factor. For instance, the installation of green roofs can only take place on buildings' roofs, whereas porous pavements can be only applied when road surfaces are available. Moreover, whether the area is privately or publicly owned represents an additional essential variable. Public areas and buildings are more easily exploitable for urban regeneration interventions. Therefore, the maximum available area to be converted into LID-BMPs can be derived through queries of land use map attributes.

2.2 Implementation of the Baseline Scenario (BS)

To properly assess the benefits deriving from the implementation of design interventions, the modelling of the non-intervention scenario (Baseline Scenario, BS) was needed, to be compared with the post-intervention ones (Design Scenarios, DSs).

The BS was developed by setting all the hydraulic and geo-morphological features of the catchment and its sections (sub-catchments). Namely, within the EPA SWMM 5.1 environment the area extension A, the equivalent width W and the permeability and soil properties were set. Then, the skeletonized sewer system was modeled, including the inflow nodes units and the outflow located at the final section of the catchment. The first node of the network, located on the upstream side of each sub-catchment was also modeled as a storage unit, i.e. assuming its operation as a stormwater detention tank, to limit the flowing rate of the downstream trunks to values reliable with their conveying capacity.

Simulations were performed by setting hyetographs related to the critical rainfall duration d, at different return periods T. Finally, the hydraulic behavior of the network was analyzed and the outfall loading volumes were estimated.

2.3 Implementation of Design Scenarios (DS) with LID-BMPs

The DSs including LID-BMPs were modeled within the SWMM 5.1 environment, according the LID Control module, defining the setting parameters of each LID, influencing the storage, the infiltration, and the outflow processes of the intercepted water.

The size of each LID was not set a priori because it was the result of the optimization procedure, carried out by combining the SWMM 5.1 hydraulic solver with the meta-heuristic HS algorithm (Geem et al. 2001). Nevertheless, the allowable minimum and maximum area of each LID were set, as a function of the spatial analysis.

2.4 Harmony Search (HS) Application

The optimization algorithm for LIDs design was based on the HS meta-heuristic algorithm. The input parameters to be included within the calculation code, derived from the spatial steps of Fig. 1, were: the range of surface area to be converted into LID A_{LID} (m^2), the construction costs C (M€), and the flooded water volume V_0 (m^3), where the subscripts 0 refers to the BS.

The HS is a meta-heuristic algorithm first developed by Geem et al. (2001) as an optimization technique capable of numerically performing a musical harmony of jazz improvisation. The harmony was finalized in a solution vector and, through optimization techniques, the numerical improvisation of a musician is performed. The aesthetic harmony evaluation is assessed through an Objective Function (OF), reaching, after a number of iterations, the perfect harmonic state. According to the original framework (Geem et al. 2001), the algorithm consists of 5 main steps:

– *Step 1: Initialization and setting of the HS parameters*, to set the required parameters: the Harmony Memory Considering Rate (HMCR), the Pitch Adjusting Rate (PAR), the Harmony Memory Size (HMS: number of solution vectors) and the ending criterion. The latter is the total number of improvisations, corresponding to the number of per-

formed iterations. The HMCR and PAR operators are set in Step 3, useful to evolve the solution vectors. When a multi-objective algorithm runs, a Pareto Front is then defined, composed of not dominated solutions, namely better (or not worse) than other ones.

– *Step 2: initialization of the Harmony Memory (HM) matrix* (Eq. (1)), composed by a number of randomly generated solution vectors $x_l{}^i = \left(x_l{}^i \; \ldots x_N{}^i\right)$ equal to HMS.

$$HM = \begin{bmatrix} x_1^1 & \cdots & x_N^1 \\ \vdots & \vdots & \vdots \\ x_1^{HMS} & \cdots & x_N^{HMS} \end{bmatrix} \begin{matrix} \rightarrow & f\left(x^1\right) \\ \vdots & \vdots \\ \rightarrow & f\left(x^{HMS}\right) \end{matrix} \tag{1}$$

– *Step 3: new improvisation of harmony from the HM matrix*, to generate a new harmony vector, by employing three operators: Memory Considerations, Pitch Adjustments and Randomization. A first decision variable (x'_i) can be selected from any value in the specified HM range ($x_i{}^1 \sim x_i{}^{HMS}$), combined with the probability of choosing a totally random value for the decision variable x'_i:

$$x'_i = \begin{cases} x'_i \in \left\{x_i^1, x_i^2, ..., x_i^{HMS}\right\} & \text{with probability } HMCR \\ x'_i \in \mathbf{X}_i & \text{with probability } (1 - HMCR) \end{cases} \tag{2}$$

where HMCR varies from 0 to 1. It is the probability to select one value from the HM, whereas (1-HMCR) is the probability to select a random feasible value, not belonging to HM. Values of the other decision variables ($x'_2,..., x'_N$) are defined with the same standard.

– *Step 4: updating the HM matrix*, as a function of the OF, whether the new harmony vector is better than the worst of the HM, by replacing the latter.

– *Step 5: application of the stopping criterion*, set in the frame of this work equal to the maximum number of iterations NI. Else, Steps 3 and 4 run again.

2.5 Hydraulic Simulation in EPA SWMM 5.1

Once the overall number of iterations was achieved, the hydraulic simulations in EPA SWMM 5.1 run to estimate the flooded water volumes *V* and assess the overall hydraulic behavior of the system, in compliance with the hydraulic constraints and the set goals.

2.6 Set of Solutions

The methodology ended by generating a set of solutions and estimating the flooded water volume *V* of each solution. The combined minimization of the overall construction costs *C* associated to each set of selected LIDs and the limitation of the flooded volume *V*, consistently with the hydraulic and technical constraints (including the maximum area convertible into each LID), was set as OF. The performance of the DS was evaluated through the performance indicator $r = V/V_0$, defined flooded volume rate.

The goodness of results was also assessed by generating the Empirical Attainment Function (EAF). It returned the boundary separating points resulting to be "attainable" (dominated according to the Pareto settlement) in at least a fraction or quantile of the simulations (López-Ibáñez et al. 2010; Fonseca et al. 2011). Thus, the EAF simplified the performance assessment of the two-objective optimization algorithm, plotting its evolution in a graphical manner.

3 The Case Study of Soccavo Catchment (Naples, Italy)

The methodological approach introduced in Sect. 2 was applied to the case study of Soccavo, a densely inhabited district in the western part of the Municipality of Naples (Italy). The study area shows a significantly high urban density and is mainly characterized by impervious areas. Processing a Digital Terrain Model (DTM) using the *Hydrology* tools of the ArcMap 10.7 software (ESRI 2010), an urban catchment of 26 ha was identified in the northern portion of Soccavo (reference to Fig. 3a), downhill to a sloped area. The catchment is crossed in the middle by a motorway linking the district to the neighbour ones. The urban structure is mainly made by residential building, built between the 1960s and the 1980s, within densely built blocks. Public spaces are almost completely missing, and a kindergarten is the only available community facility. Nevertheless, private gardens, playground and rural areas contribute to enhance the rate of unsealed soils in the study area (Fig. 3).

The case study was investigated by processing a geographic database provided by Campania Region and achieved from the 2011 Regional Technical Map (scale 1:5.000, CRS ETRS2000 UTM-33 N). The geographic database was made of polygon feature classes, corresponding to different land uses, and by a DTM with 1 m spatial resolution (Fig. 4a). A 0.40 m resolution 3-band orthophoto, provided by the Italian Agricultural Payment Agency (AGEA) in 2014, was then applied.

A polyline shapefile was employed to design the drainage system: for each edge, detailed information concerning pipe typology, size, length, slope and laying surface
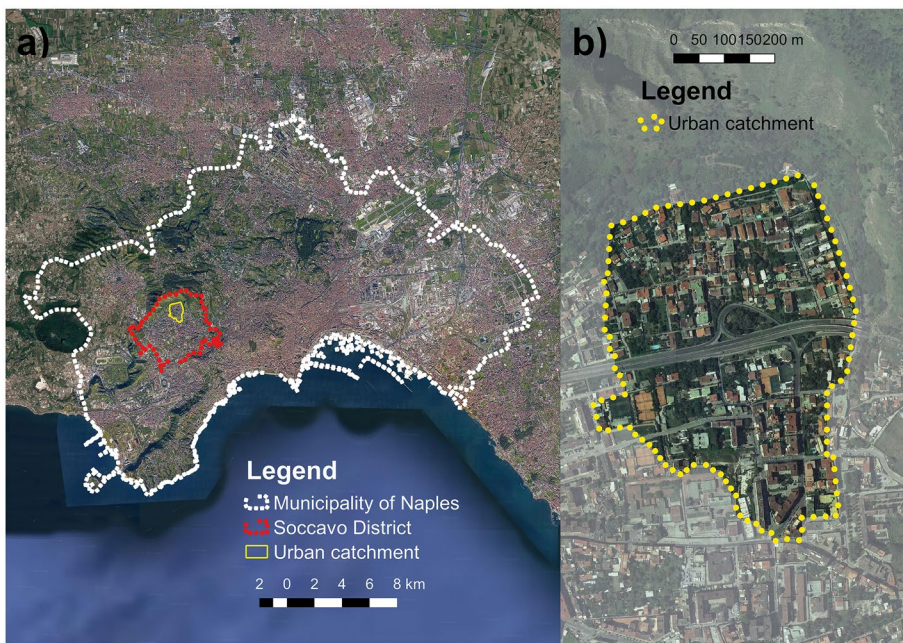

Fig. 3 **a** Municipality, district and urban catchment boundaries overlayed on a Satellite Imagery of Naples Gulf; **b** Urban catchment boundary overlaid on an aerial orthophoto
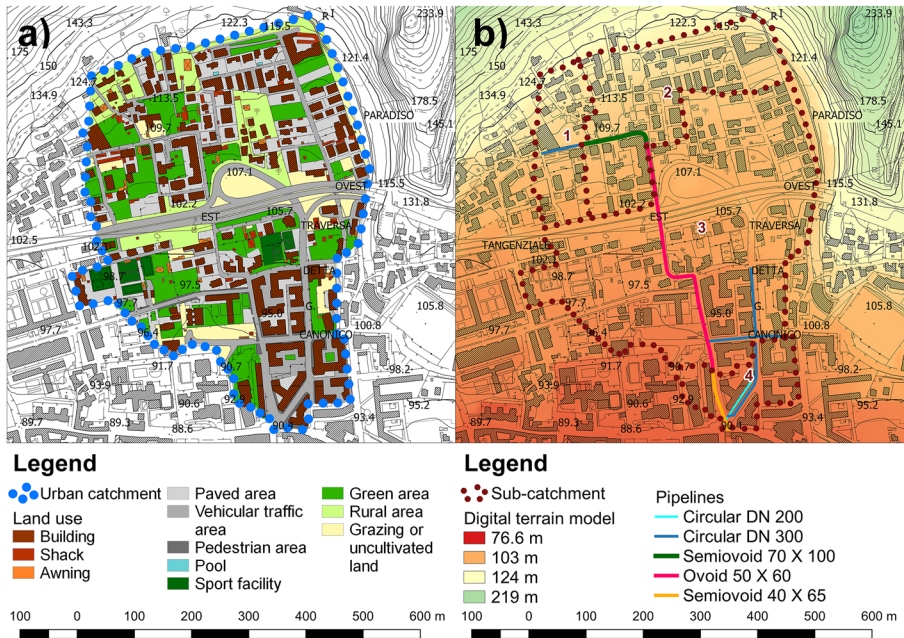
Fig. 4 **a** Geographic database categorized by land uses; **b** Sub-Catchments borders and drainage network, categorized by pipelines typology, overlaid with digital terrain model

height were provided. From the analysis of the sewer system, 4 sub-catchments were identified and serially numbered from north to south (Fig. 4b).

The Sub-Catchment 1 (2.37 ha) is served by a DN300 circular pipeline lying under a local road; the sewer system of the Sub-Catchment 2 (6.20 ha) presents a 70×100 mm semi-ovoid pipeline, instead. Sub-Catchment 3, the largest one (15.55 ha), is mainly served by a 50×60 mm ovoid pipeline, whereas few dwellings located in the eastern part of the sub-catchment are supplied by a DN300 pipeline. The Sub-Catchment 4, the smallest one (1.97 ha), is mainly served by a 40×65 mm semi-ovoid pipeline and the settlements placed in the eastern part of the sub-catchment are supplied by a DN300 pipeline. It is worth noting that, differently from a technically effective design, the diameters of downstream branches are smaller than the upstream ones, making the sewer system ineffective and particularly susceptible to failure under extreme rainfall events. For such system, the proper design of LID-BMPs may provide a significant reduction of the runoff volumes discharged into the drainage system, reducing the flood risk.

3.1 Territorial Analysis of Soccavo (IT) Catchment

The territorial analysis started by processing the 3-band orthophoto using ArcGis Pro software, using the Band IDs method for band extraction. The unsupervised method was adopted for image segmentation by setting three parameters: (1) spectral detail, to categorize spectral differences between pixels, ranging from 1 to 20 and set equal to 13; (2) spatial detail, to classify the proximity between pixels, ranging from 1 to 20 and set equal to

5; (3) minimum segment size in pixel, to provide a threshold below which segment with fewer pixels are merged into a neighbouring segment, set equal to 100.

Moreover, the classification method was set as object-based: it gathered neighbouring pixels together, based on how similar they were, in terms of colour and shape properties. The classification was performed using an ISO Cluster classifier, adopting the K-mean method. The maximum number of iterations was set equal to 50.

To validate the classification, 200 accuracy assessment points were randomly generated, equally distributed among impervious and pervious areas. Relative to the confusion matrix, 96 pixels out of 100 were correctly classified as impervious and after the validation procedure, 16 pixels were re-classified as impervious. Thus, the Kappa index, measuring the classification accuracy, was equal to 80%. Given the high spatial and spectral variability of the processed orthophoto, this value was considered reliable enough for the aim of this study.

Once the permeability map was got, the automated tool, created using the ArcMap Model Builder to calculate the sub-catchments data required for hydraulic simulations, run. It was made of 3 sub-models: (1) the slope computing, which processed the DTM to assign the mean slope value to each Sub-Catchment polygon feature; (2) the imperviousness rate computing, which processed the permeability map achieved in the previous step to assign the imperviousness rate to each Sub-Catchment polygon feature; (3) the width computing, which processed the sub-catchment polygon features and the drainage network polylines to achieve the mean width of each Sub-Catchment.

Outcomes of the automated model are synthetized in Table 1. Sub-Catchments 1 and 2 were nearly twice as sloping as Sub-Catchments 3 and 4. The imperviousness rates were always higher than 50%, peaking at 82% in Sub-Catchment 4.

Finally, the land use map was reclassified to assess the maximum extension of areas prone to implement each LID-BMP measure. Each polygon in the geographic database was re-classified either as public or as private.

In Fig. 5 the graphical framework of the procedure of the area categorization is given, whereas in Table 1 the results of the territorial analysis are summarized.

4 Results and Discussion

From the GIS spatial analysis described in Sect. 3, public roads, except for the motorway and its junctions, were made potentially available to be converted into porous pavements. Footpaths and public open spaces were equally converted into bio-retention areas and porous pavements, instead. The flat roof of the kindergarten was made available as a green roof (Table 2; Fig. 6). Multiple DSs were defined by varying the LID area A_{LID} and keeping fixed the type of measures to be implemented. It is worth mentioning that the area convertible into LIDs was about the 17% of the overall catchment area.

	Sub-Catchment	Area A [m^2]	Width W [m]	Slope s [%]	Imperviousness rate $\%IMP$ [%]
Table 1 Territorial analysis results of each Sub-Catchment	1	23′717.10	339.46	14.20	0.52
	2	62′010.84	478.59	11.08	0.58
	3	155′513.95	347.21	7.36	0.56
	4	19′730.87	189.39	7.49	0.82

Confusion matrix

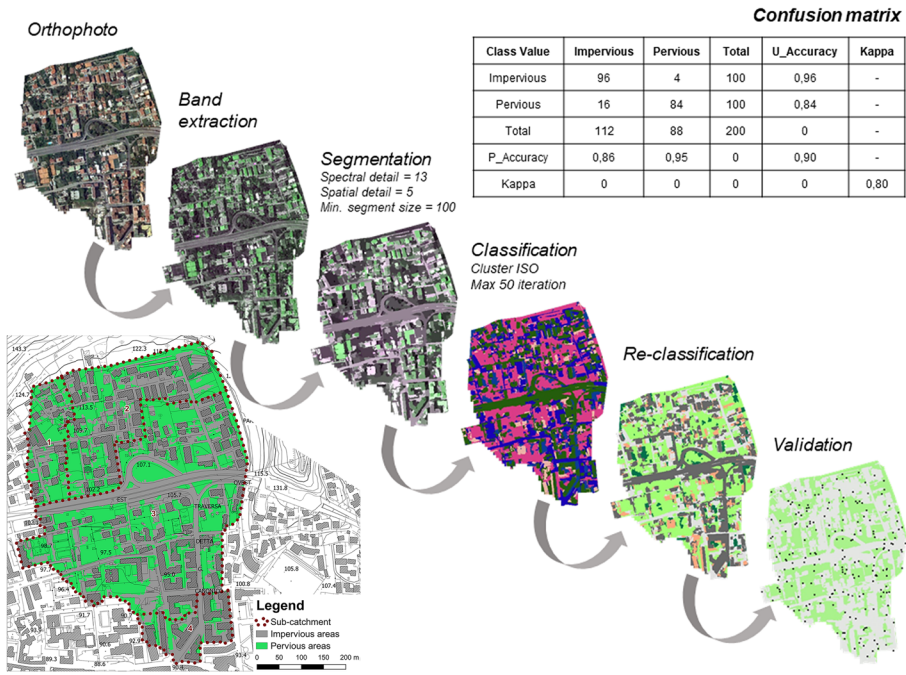| Class Value	Impervious	Pervious	Total	U_Accuracy	Kappa
Impervious	96	4	100	0,96	-
Pervious	16	84	100	0,84	-
Total	112	88	200	0	-
P_Accuracy	0,86	0,95	0	0,90	-
Kappa	0	0	0	0	0,80

Fig. 5 Schematic representation of the procedure implemented for the classification of impervious and pervious areas in the study area

The identified DSs were tested and, by applying the HS algorithm, the best trade-off between the flooding volume V reduction and the construction costs C was identified. Moreover, to detain a share of the (or the whole) flooded volume, the introduction of stormwater detention tanks was also considered at the initial node of each sub-catchment. The unitary cost c_T (€/m^2) of tank was estimated via market surveys, as a function of the tank area E (m^2), according to Eq. (3):

$$c_T = 820.41 \cdot E - 856.46 \tag{3}$$

Equation (3) remarks how the implementation of hybrid solutions, using stormwater tanks, significantly increased the construction costs with respect to the LID scenario.

Table 2 Maximum extension of areas potentially available for the selected LID-BMP technologies in each sub-catchment

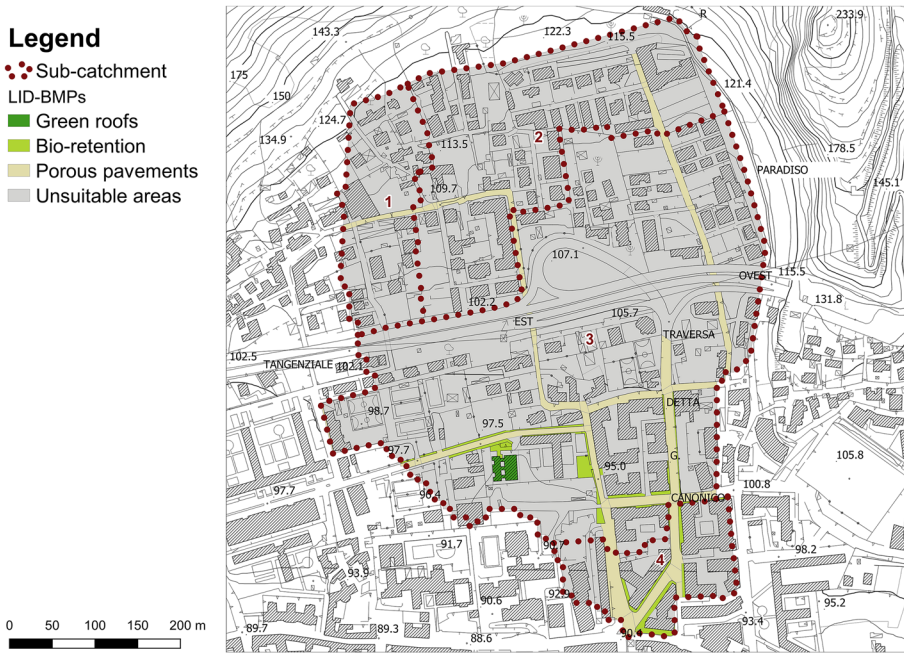| LID-BMP	Area A_{LID} [m^2]				
	Sub-Catchment 1	Sub-Catchment 2	Sub-Catchment 3	Sub-Catchment 4	Total Catchment
Bio-Retention	0	0	1'217	673	1'890
Green Roofs	0	0	728	0	728
Porous Pavements	484	1'722	12'514	4'515	19'234
Total	484	1'722	14'459	5'188	21'852

Fig. 6 Areas available for the implementation of the selected LID-BMPs

From a preliminary assessment, a rectangular hyetograph with critical duration $d = 1$ h was employed for simulations. Constant rainfall intensities i of 33.17, 44.91 and 53.89 mmh^{-1} were set for three return periods T of 5, 20 and 50 years, respectively.

HMS, HMCR, PAR and NI parameters of the Harmony Search were set equal to 40, 0.50, 0.05 and 20000, respectively, whereas the construction costs were estimated following Zhang et al. (2013), as a function of the discounted construction unitary costs of Table 3.

The dynamic wave and the Curve Number were set in EPA SWMM 5.1 as routing and infiltration models, respectively. Table 4 reports the main LIDs parameters set within EPA SWMM 5.1.

The optimal solutions composing the Pareto Front are plotted in Fig. 7 for the three simulated return periods T. It shows the correlation between LIDs construction costs and the flooded volume rate $r = V/V_0$. With increasing the construction costs, a significant reduction of the flooding volume was observed, reaching a reduction as high as 80% (flooded volume rate $r = 20\%$) for construction costs of about 1.0 M€, 1.4 M€ and 1.6 M€ at $T = 5$, 20 and 50 years, respectively.

Table 3 Discounted construction unitary costs

LID	Unitary Costs [€/m^2]
Bio-Retention	92.70
Green Roofs	231.82
Porous Pavements	218.05

Table 4 Set of parameters of LIDs in EPA SWMM 5.1

LID	Bio-Retention	Green Roofs	Porous Pavements
Surface Berm Height [m]	0.20	0.20	0.20
Soil Thickness [m]	0.60	0.10	0.20
Storage Thickness [m]	0.30	0.50	0.30
Storage Void Ratio [-]	0.75	0.60	0.75
Manning Surface Roughness [$sm^{-1/3}$]	0.40	0.15	0.10

Figure 7 shows that, for all the three return periods, r decreased almost linearly at increasing the design cost C in the range from 5 to 97%. Whereas a significant C increase was observed outer this range, making evidence of the need of developing hybrid scenarios to nullify the flooded volume r.

The EAF for the three return periods is plotted in Fig. 8. The median EAF was the function having an attainable point rate of 50%, showing the evolutionary capability of the HS to provide solutions able to simultaneously satisfy the two objectives: the construction costs C and the flooding volume rate r reduction. Indeed, the trend of the median EAF is highly comparable with the Pareto Front's, resulting in a remarkable outcome for the effective convergency of the implemented algorithm.

In Fig. 9, the non-linear increase of construction costs at increasing the return period T is plotted with reference to solutions that completely prevent flooding events
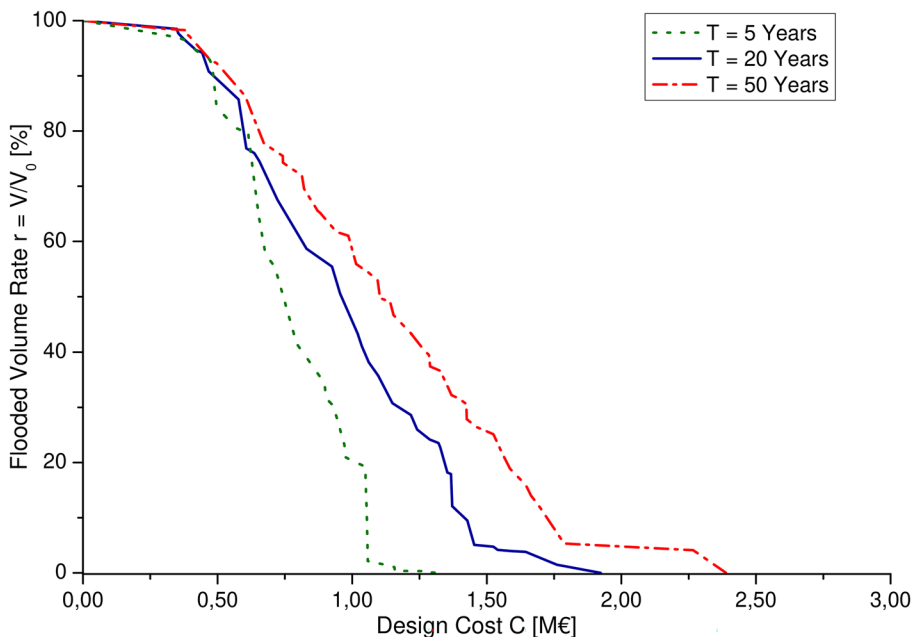
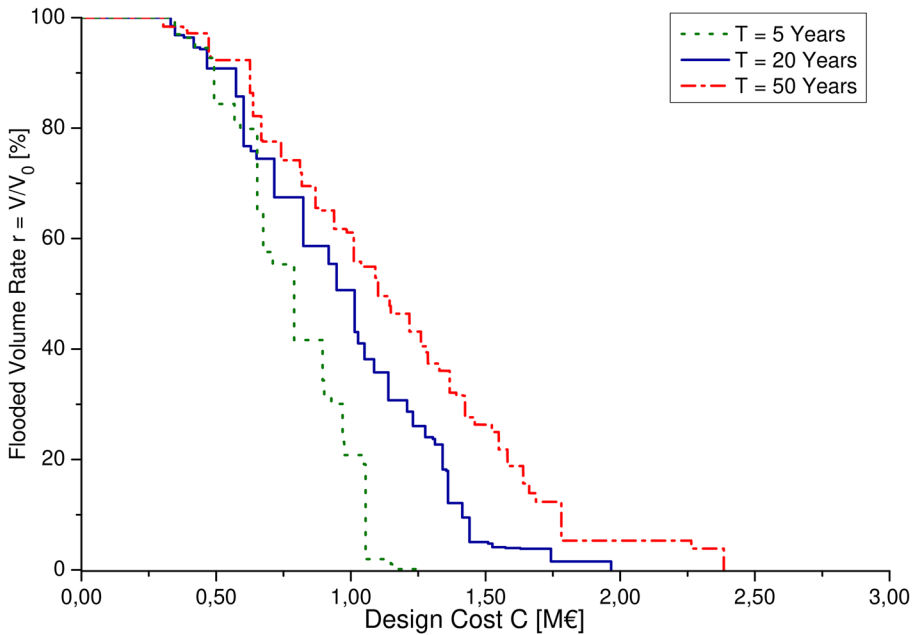**Fig. 7** Pareto front of the optimal solutions for return period $T = 5$, 20 and 50 years

Fig. 8 Empirical Attainment Function (EAF) for $T = 5, 20, 50$ years

($r = 0\%$). Specifically, the minimum cost was equal to 1.34 M€, 1.92 M€ and 2.39 M€ for $T = 5$, 20, 50 years, respectively. The following correlation between T and C was thus derived:
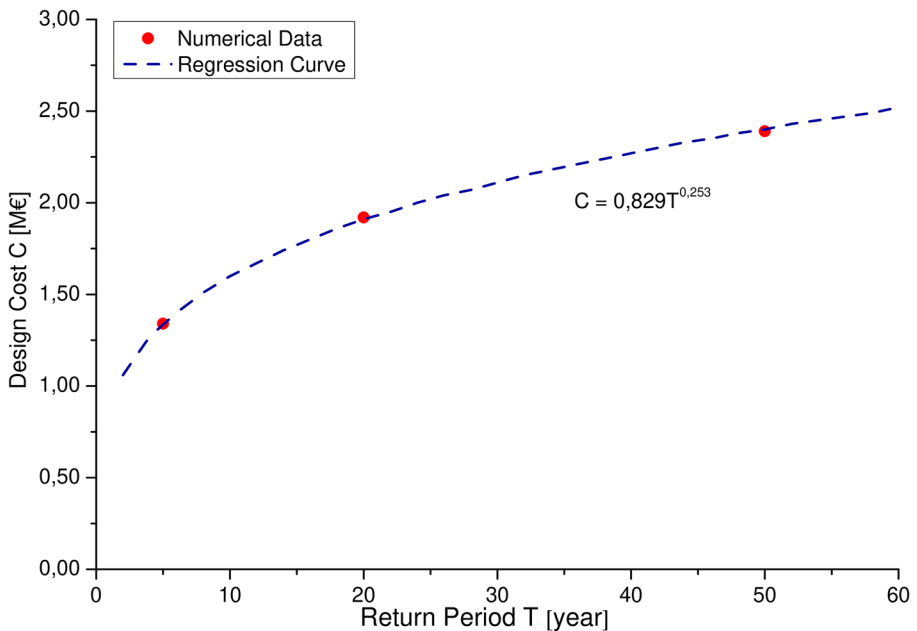

$$C = 0{,}829T^{0{,}253}$$

Fig. 9 Construction cost-return period correlation for $T = 5, 20$ and 50 years

$$C = 0.829 \cdot T^{0.253} \tag{4}$$

For the sake of completeness, simulations were then performed at $T = 40$ years, observing a reliable trend with Eq. (4). Whereas for $T = 2$ years greater discrepancies were observed because, given the limited flooded volume at the baseline scenario, the benefits of LIDs were less significant.

The severe undersizing of the sewer system in the study area led to the choice to not limiting the maximum volume of the stormwater tank in the DSs definition. Thus, results from the optimization allowed detecting the sub-catchments most susceptible to flood risk and enabled to identify the location of the stormwater tanks in the related initial node, in order to limit the flowing rates within the downstream sub-catchment sewer system.

From the optimization procedure, and for all the considered return periods T (Table 3), stormwater tanks resulted to be required only for Sub-Catchments 1 and 3, whereas they were not needed for Sub-Catchments 2 and 4.

In Fig. 10 the maximum volumes of the stormwater tanks W_T are plotted for Sub-Catchments 1 and 3. As observed for the construction costs, at increasing the return period T, the maximum volume of stormwater tanks W_T increased with a non-linear trend, according to Eqs. (5) and (6) for Sub-Catchments 1 and 3, respectively.

$$W_{T1} = 199.4 \cdot T^{0.310} \tag{5}$$
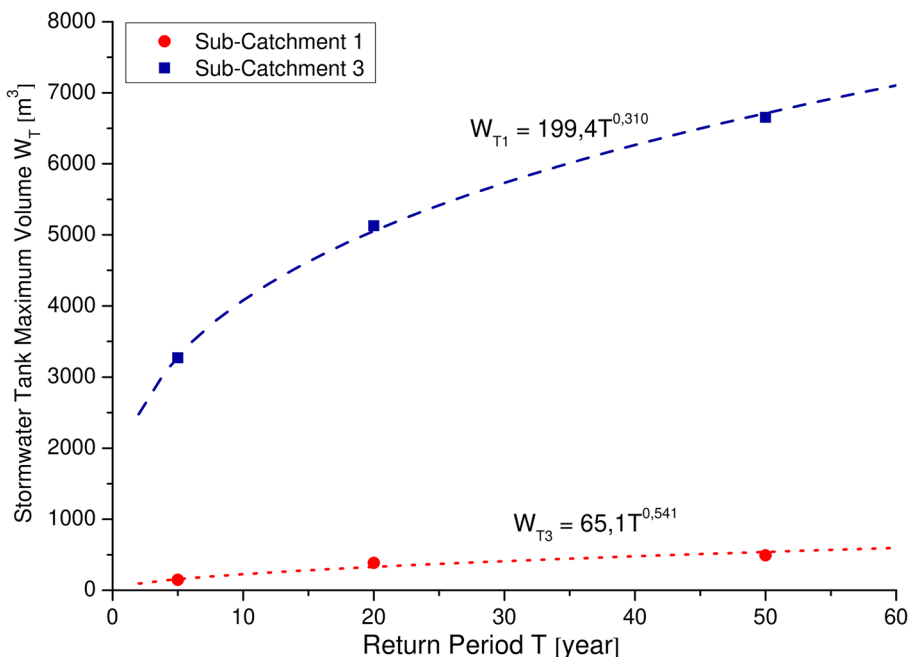
$$W_{T3} = 65.1 \cdot T^{0.541} \tag{6}$$

Fig. 10 Maximum volumes W_T of stormwater tanks in critical nodes at varying the return period T

Table 5 Design of LID practices and stormwater tanks of 4 Sub-Catchments ($r=0$ solution)

	T = 5 years				T = 20 years				T = 50 years			
Sub-Catchment	1	2	3	4	1	2	3	4	1	2	3	4
Bio-Retention Area [m²]	0	0	440	470	0	0	297	350	0	0	172	215
Green Roof Area [m²]	0	0	238	0	0	0	389	0	0	0	569	0
Porous Pavement Area [m²]	411	667	630	344	452	305	835	289	484	346	2′491	1′420
Stormwater Tank Volume [m³]	146	0	3′275	0	386	0	5′129	0	491	0	6′656	0

As observed by De Paola et al. (2018), the installation of stormwater tanks is recommended in presence of improperly designed urban drainage system, such as when the trunk diameter decreases moving downstream in the drainage system, as observed in the case study analyzed herein (Fig. 4).

The implementation of a hybrid solution, combining LIDs with stormwater tanks, allowed voiding the flooded volume with $r=0\%$, defining the final DS of this study, as per the optimal design given in Table 5. In Sub-Catchment 3 the stormwater tank had a significant volume, of 3′275, 5′129 and 6′656 m³ at $T=5$, 20 and 50 years, respectively. Nevertheless, the territorial analysis proved the feasibility of its insertion, by converting public spaces to this purpose (Fig. 11). The DS provided the reduction of the number of pressurized trunks, even when high intensity events occur.

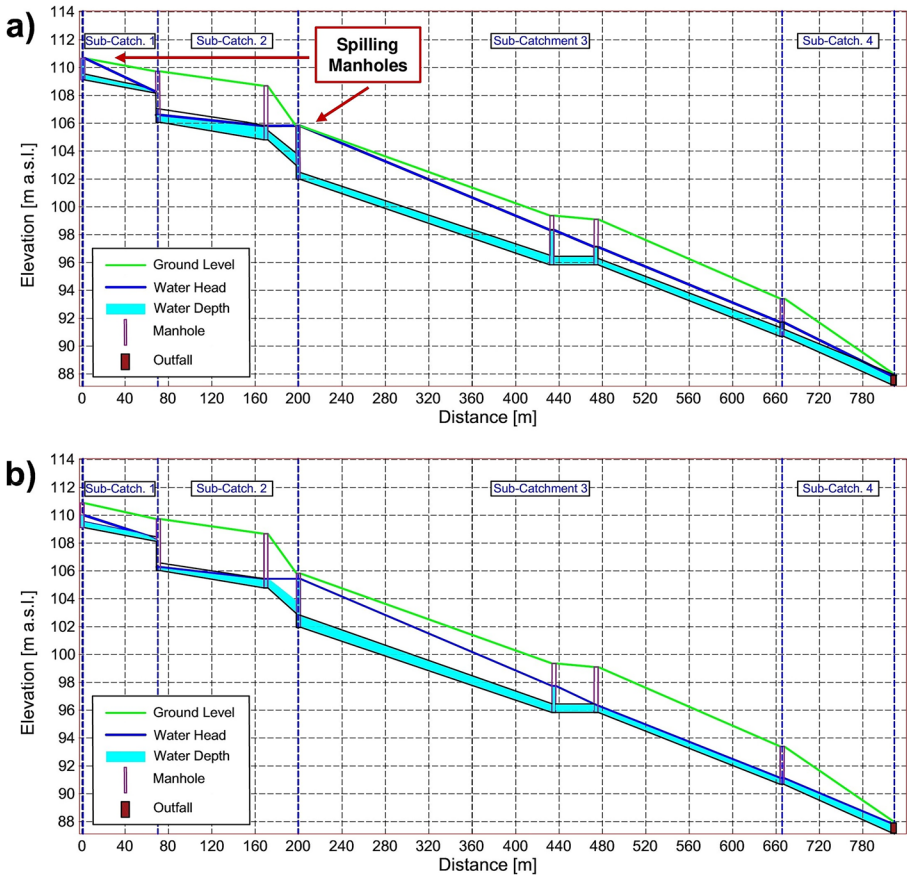**Fig. 11** Areas converted into LID-BMPs and location of stormwater detention tank of Sub-Catchment 3

Fig. 12 Backwater profile ($d=1$ h and $T=5$ years) for **a** BS and **b** DS

To better assess the benefits of flooding reduction deriving from the DS with LIDs, in Fig. 11 the profile of the main trunks of the whole sewer system in the study area is plotted for $T=5$ years for the BS (Fig. 12a) and the DS (Fig. 12b). The reduction of flowing is observable within the system, by significantly limiting the filling rate of each trunk and manhole. Indeed, the upstream manholes experiencing spilling events at the BS, presented lower filling rate at the DS.

In Fig. 13 the comparison between the inlet Q_{in} (solid line) and the outlet flow rate Q_{out} (dashed line) of the stormwater tank for Sub-Catchment 3 is plotted for the three return periods. It shows the reliability of the implemented interventions in reducing the peak flow rate at the initial section of the sub-catchment, observing the reduction of the peak flow rate of the 17%, 37% and 49%, for $T=5$, 20 and 50 years, respectively.

Conversely, at the outfall node of the system, a slight reduction of the peak flow was observed, varying from about the 2% to 4% for the three return periods (Fig. 14).

Nevertheless, it is worth noting that the primary goal of the DS was lowering the flooded volume, which was completely nullified with this solution.
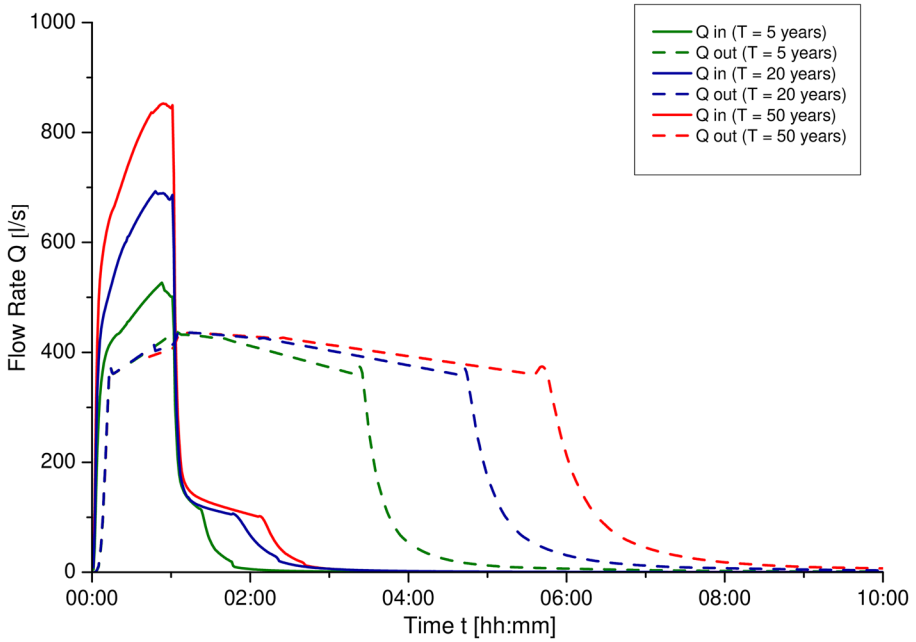
Fig. 13 Comparison between the inlet and outlet hydrographs of the stormwater tank of Sub-Catchment 3
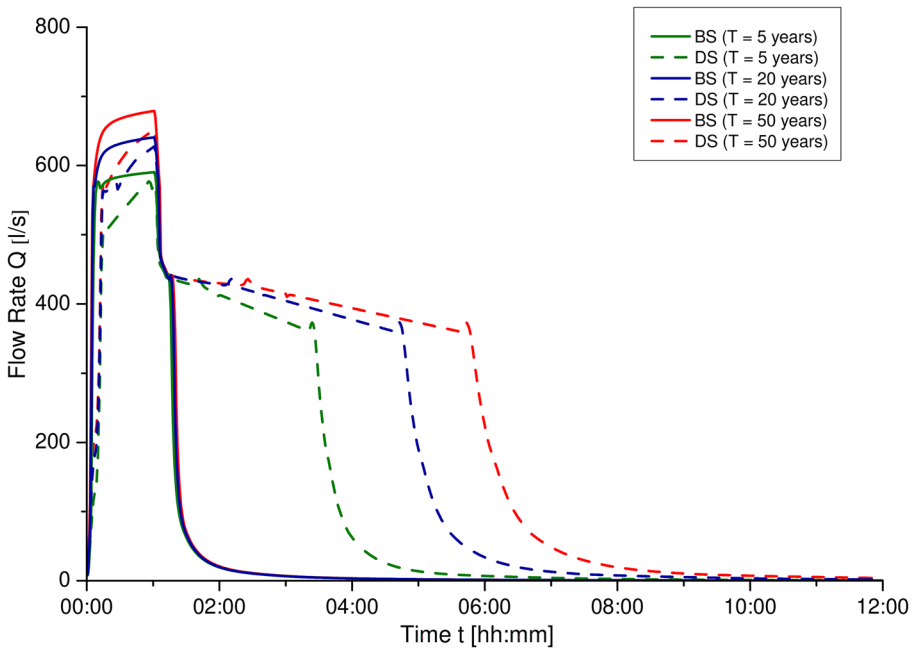

Fig. 14 Comparison of hydrographs at the outfall node between BS and DS

5 Conclusions

This paper aims to 1) propose a multidisciplinary methodological approach for increasing the urban resilience to extreme meteorological events through the implementation of a LID-BMPs; 2) provide an integrative model, based on the integration of GIS spatial analysis with both a hydraulic solver and a optimization procedure for the optimal design of LID-BMPs scenarios; 3) test the reliability of the proposed approach on the case study of the urban catchment of Soccavo (Naples, Italy).

The novelty of the proposed model mainly lies in the integration of spatial GIS processing with the Harmony Search meta-heuristic optimization model and the EPA SWMM5.1 hydraulic solver. Indeed, the spatial analysis in GIS environment was automated through in-house routines capable to process the input data of the hydraulic simulations and the solution optimization.

The proposed methodology can be thus intended as a Decision Support System (DSS) for a multi-objective design of urban regeneration interventions, with a specific focus on the optimal management of water systems. Indeed, the optimal extension of the area to be converted into LID-BMPs can be obtained by fixing as a constraint the economic budget available for the intervention, while respecting constraints on the technical and hydraulic feasibility of the measures. Alternatively, the tool can be used to assess the minimum budget to be allocated for achieving a desired reduction of flooded volumes and, in turn, of flood risk.

With reference to the Soccavo (Italy) case study, the territorial analysis allowed identifying the most effective size of measures to enhance the urban resilience against extreme weather events and flooding risk, given the territorial, technical and economic constraints. Specifically, the spatial analysis allowed selecting the most relevant solutions, namely the bio-retention systems, porous pavements and green roofs and to set the maximum available area to be converted into each LID. The optimization procedure, coupled with the hydraulic simulations, provided for the optimal LID design, able to reduce the flooding volume of about the 80%. Moreover, a hybrid scenario, got by coupling LIDs with stormwater detention tanks, provided the zeroing of flooded volumes and the decrease of flowing rate within the drainage system, even under extreme events.

Moreover, the outcomes highlighted the non-linear dependency of construction costs and maximum volumes of stormwater tanks with the return period, useful for a preliminary cost–benefit assessment of the intervention.

Testing and adapting the proposed methodology to case studies where different LID-BMPs can be selected and in presence of more complex drainage systems represent a challenging development of the present research and is currently ongoing.

Declarations

Ethical Approval The authors declare that the manuscript has not been submitted to other journals. The submitted work is original and not published elsewhere. This study is not split up into several parts.

Consent to Participate Not applicable.

Consent to Publish Not applicable.

Competing Interests All authors certify that they have no affiliations with or involvement in any organization or entity with any financial interest or non-financial interest in the subject matter or materials discussed in this manuscript.

References

Bishop YM, Holland PW, Fienberg SE (2007) Discrete multivariate analysis theory and practice

Blick SA, Kelly F, Skupien JJ (2004) New Jersey stormater best management practices manual

Booth DB (1991) Urbanization and the natural drainage system.pdf. Northwest Environ J 93–118

Carter JG, Cavan G, Connelly A et al (2015) Climate change and the city: Building capacity for urban adaptation. Prog Plann. https://doi.org/10.1016/j.progress.2013.08.001

De Paola F, Giugni M, Pugliese F, Romano P (2018) Optimal design of LIDs in urban stormwater systems using a harmony-search decision support system. Water Resour Manag. https://doi.org/10.1007/s11269-018-2064-8

Dietz ME (2007) Low impact development practices: A review of current research and recommendations for future directions. Water Air Soil Pollut

ESRI (2010) ArcGIS, Version 10.1. ESRI, Redlands California, USA

Fletcher S, Lickley M, Strzepek K (2019) Learning about climate change uncertainty enables flexible water infrastructure planning. Nat Commun 10:1–11. https://doi.org/10.1038/s41467-019-09677-x

Fletcher TD, Shuster W, Hunt WF et al (2015) SUDS, LID, BMPs, WSUD and more – The evolution and application of terminology surrounding urban drainage. Urban Water J. https://doi.org/10.1080/1573062X.2014.916314

Fonseca CM, Guerreiro AP, López-Ibáñez M, Paquete L (2011) On the computation of the empirical attainment function. In Lecture Notes in Computer Science (including subseries Lecture Notes in Artificial Intelligence and Lecture Notes in Bioinformatics)

Forsee WJ, Ahmad S (2011) Evaluating urban storm-water infrastructure design in response to projected climate change. J Hydrol Eng 16:865–873. https://doi.org/10.1061/(asce)he.1943-5584.0000383

Geem ZW, Kim JH, Loganathan GV (2001) A new heuristic optimization algorithm: Harmony search. Simulation. https://doi.org/10.1177/003754970107600201

Hou J, Zhu M, Wang Y, Sun S (2020) Optimal spatial priority scheme of urban LID-BMPs under different investment periods. Landsc Urban Plan. https://doi.org/10.1016/j.landurbplan.2020.103858

Jia H, Lu Y, Yu SL, Chen Y (2012) Planning of LID-BMPs for urban runoff control: The case of Beijing Olympic Village. Sep Purif Technol

Khan S, Lau SL, Kayhanian M, Stenstrom MK (2006) Oil and grease measurement in highway runoff - Sampling time and event mean concentrations. J Environ Eng. https://doi.org/10.1061/(ASCE)0733-9372(2006)132:3(415)

Liu Y, Cibin R, Bralts VF et al (2016) Optimal selection and placement of BMPs and LID practices with a rainfall-runoff model. Environ Model Softw. https://doi.org/10.1016/j.envsoft.2016.03.005

López-Ibáñez M, Paquete L, Stützle T (2010) Exploratory analysis of stochastic local search algorithms in biobjective optimization. Exp Methods Anal Optim Algorithms

Nie L, Lindholm O, Lindholm G, Syversen E (2009) Impacts of climate change on urban drainage systems - a case study in Fredrikstad, Norway. Urban Water J 6:323–332. https://doi.org/10.1080/15730620802600924

Pignalosa A, Silvestri N, Pugliese F et al (2022) Long-term simulations of nature-based solutions effects on runoff and soil losses in a flat agricultural area within the catchment of LakeMassaciuccoli (Central Italy). Agric Water Manag 273:107870. https://doi.org/10.1016/J.AGWAT.2022.107870

Pugliese F, Caroppi G, Zingraff-Hamed A et al (2022) Assessment of NBSs effectiveness for flood risk management: The Isar River case study. Aqua Water Infrastruct Ecosyst Soc 71:42–61. https://doi.org/10.2166/aqua.2021.101

Raei E, Reza Alizadeh M, Reza Nikoo M, Adamowski J (2019) Multi-objective decision-making for green infrastructure planning (LID-BMPs) in urban storm water management under uncertainty. J Hydrol. https://doi.org/10.1016/j.jhydrol.2019.124091

Recanatesi F, Petroselli A, Ripa MN, Leone A (2017) Assessment of stormwater runoff management practices and BMPs under soil sealing: A study case in a peri-urban watershed of the metropolitan area of Rome (Italy). J Environ Manag. https://doi.org/10.1016/j.jenvman.2017.06.024

Rosenzweig C, Solecki W, Romero-Lankao P et al (2015) ARC3.2. Summary for city leaders. Clim Chang Cities, Second Assess Report Urban Clim Res Netw (UCCRN), Columbia Univ. https://doi.org/10.1080/23298758.1994.10685604

Rossman LA (2015) Storm water management model user's manual version 5.1. Natl Risk Manag Lab Off Res Dev United States Environ Prot Agency, Cincinnati, Ohio

Špitalar M, Gourley JJ, Lutoff C et al (2014) Analysis of flash flood parameters and human impacts in the US from 2006 to 2012. J Hydrol. https://doi.org/10.1016/j.jhydrol.2014.07.004

Schreurs MA, Tiberghien Y (2007) Multi-level reinforcement: Explaining European Union leadership in climate change mitigation. Glob Environ Polit

Wurzel RKW, Connelly J (2010) The European Union as a leader in international climate change politics

Xu T, Jia H, Wang Z et al (2017) SWMM-based methodology for block-scale LID-BMPs planning based on site-scale multi-objective optimization: a case study in Tianjin. Front Environ Sci Eng. https://doi.org/10.1007/s11783-017-0934-6

You L, Xu T, Mao X, Jia H (2019) Site-scale LID-BMPs planning and optimization in residential areas. J Sustain Water Built Environ. https://doi.org/10.1061/JSWBAY.0000870

Zanandrea F, Silveira ALLD (2018) Effects of LID implementation on hydrological processes in an urban catchment under consolidation in Brazil. J Environ Eng (United States). https://doi.org/10.1061/(ASCE)EE.1943-7870.0001417

Zhang G, Hamlett JM, Reed P, Tang Y (2013) Multi-objective optimization of low impact development designs in an urbanizing watershed. Open J Optim. https://doi.org/10.4236/ojop.2013.24013

Publisher's Note Springer Nature remains neutral with regard to jurisdictional claims in published maps and institutional affiliations.

Authors and Affiliations

Francesco Pugliese[1] · **Carlo Gerundo[2]** · **Francesco De Paola[1]** · **Gerardo Caroppi[3]** · **Maurizio Giugni[1]**

Carlo Gerundo
carlo.gerundo@unina.it

Francesco De Paola
depaola@unina.it

Gerardo Caroppi
gerardo.caroppi@aalto.fi

Maurizio Giugni
giugni@unina.it

[1] Department of Civil, Environmental and Architectural Engineering, University of Naples Federico II, Via Claudio 21, 80125 Naples, Italy

[2] Department of Civil, Environmental and Architectural Engineering, University of Naples Federico II, Piazzale Tecchio 80, 80125 Naples, Italy

[3] Department of Built Environment, Aalto University School of Engineering, Tietotie 1 E, 02150 Espoo, Finland